THE JOURNAL OF BIOLOGICAL CHEMISTRY VOL. 282, NO. 3, pp. 2116–2123, January 19, 2007

Highly Conserved Residues Asp-197 and His-250 in Agp1 Phytochrome Control the Proton Affinity of the Chromophore and Pfr Formation*[S]

Received for publication, September 15, 2006, and in revised form, November 14, 2006 Published, JBC Papers in Press, November 22, 2006, DOI 10.1074/jbc.M608878200

David von Stetten[‡1], Sven Seibeck[§1], Norbert Michael[¶], Patrick Scheerer[‖], Maria Andrea Mroginski[‡], Daniel H. Murgida[‡], Norbert Krauss[‖], Maarten P. Heyn[§], Peter Hildebrandt[‡2], Berthold Borucki[§3], and Tilman Lamparter[¶4]

From the [‡]Institut für Chemie, Technische Universität Berlin, Sekretariat PC14, Strasse des 17 Juni 135, D-10623 Berlin, [§]Fachbereich Physik, Institut für Experimentalphysik, Freie Universität Berlin, Arnimallee 14, D-14195 Berlin, [¶]Pflanzenphysiologie, Freie Universität Berlin, Königin Luise Strasse 12-16, D-14195 Berlin, and [‖]Institut für Biochemie, Charité-Universitätsmedizin Berlin, Proteinstrukturforschung, Campus Charité-Mitte, Monbijoustrasse 2, D-10117 Berlin, Germany

The mutants H250A and D197A of Agp1 phytochrome from *Agrobacterium tumefaciens* were prepared and investigated by different spectroscopic and biochemical methods. Asp-197 and His-250 are highly conserved amino acids and are part of the hydrogen-bonding network that involves the chromophore. Both substitutions cause a destabilization of the protonated chromophore in the Pr state as revealed by resonance Raman and UV-visible absorption spectroscopy. Titration experiments demonstrate a lowering of the pK_a from 11.1 (wild type) to 8.8 in H250A and 7.2 in D197A. Photoconversion of the mutants does not lead to the Pfr state. H250A is arrested in a meta-Rc-like state in which the chromophore is deprotonated. For H250A and the wild-type protein, deprotonation of the chromophore in meta-Rc is coupled to the release of a proton to the external medium, whereas the subsequent proton re-uptake, linked to the formation of the Pfr state in the wild-type protein, is not observed for H250A. No transient proton exchange with the external medium occurs in D197A, suggesting that Asp-197 may be the proton release group. Both mutants do not undergo the photo-induced protein structural changes that in the wild-type protein are detectable by size exclusion chromatography. These conformational changes are, therefore, attributed to the meta-Rc → Pfr transition and most likely coupled to the transient proton re-uptake. The present results demonstrate that Asp-197 and His-250 are essential for stabilizing the protonated chromophore structure in the parent Pr state, which is required for the primary photochemical process, and for the complete photo-induced conversion to the Pfr state.

Phytochromes are photoreceptors of plants, bacteria, and fungi that are most sensitive in the red and far-red region of the visible spectrum (1). Three different bilin chromophores are incorporated into phytochromes: plants utilize phytochromobilin and cyanobacteria use phycocyanobilin (PCB),[5] whereas other bacteria and fungi incorporate biliverdin (BV), the evolutionarily most ancient chromophore (2). In all phytochromes, the bilin is covalently attached via its ring *A* ethylidene (phytochromobilin/PCB) or vinyl (BV) side chain to a cysteine residue. The position of this cysteine, however, is different in the BV binding and the phytochromobilin/PCB binding species and is located close to the N terminus and in the GAF domain of the protein, respectively (2). Phytochromes are photochromic pigments that, upon light absorption, can be reversibly switched between the physiologically inactive and the active form. These two forms are denoted according to the absorption maxima as red-absorbing form Pr and far-red absorbing form Pfr. Upon light absorption in the Pr state, the tetrapyrrole chromophore undergoes a double bond $Z \rightarrow E$ isomerization at the *C-D* methine bridge to yield the photoproduct lumi-R, which thermally relaxes via several meta intermediate states to the Pfr form (3).

So far, most of the knowledge about the reaction mechanism of the photoconversion and about the underlying structural changes has been provided by spectroscopic studies. Only recently the first three-dimensional structure of a phytochrome has been determined (4). The structure, which refers to the Pr state of the chromophore binding domain (CBD) of DrBphP, a BV binding phytochrome from *Deinococcus radiodurans*, allows identification of the amino acids that are critical for protein-chromophore interaction. Because these amino acids are well conserved among the different phytochrome sequences, one may expect common structural motifs for the chromophore binding pockets and similar reaction mechanisms for all phytochromes. In the CBD of DrBphP, the chromophore adopts a *ZZZssa* geometry, corresponding to the *Z* configuration for all methine bridge double bonds and a *syn* conforma-

* This work was supported by the Deutsche Forschungsgemeinschaft, Sfb 498 (to M. A. M., P. H., N. K., and T. L.) and Bo 1911/1-1 (to B. B. and M. P. H.). The costs of publication of this article were defrayed in part by the payment of page charges. This article must therefore be hereby marked "*advertisement*" in accordance with 18 U.S.C. Section 1734 solely to indicate this fact.

[S] The on-line version of this article (available at http://www.jbc.org) contains supplemental Figs. S1–S4.

[1] Both authors contributed equally to this work.
[2] To whom correspondence may be addressed. Tel.: 49-30-314-21419; E-mail: hildebrandt@chem.tu-berlin.de.
[3] To whom correspondence may be addressed. Tel.: 49-30-838-54458; E-mail: borucki@physik.fu-berlin.de.
[4] To whom correspondence may be addressed. Tel.: 49-30-838-54918; E-mail: lamparte@zedat.fu-berlin.de.

[5] The abbreviations used are: PCB, phycocyanobilin; Agp1, *Agrobacterium* phytochrome 1; BV, biliverdin; Pr, red-absorbing form of phytochrome; Pfr, far-red absorbing form of phytochrome; CBD, chromophore binding domain; RR, resonance Raman; ip, in-plane.

Supplemental Material can be found at: http://www.jbc.org/cgi/content/full/M608878200/DC1

tion for the *A-B* and *B-C* bridges, whereas the *C-D* methine bridge single bond is in the *anti* conformation. Except for the *syn* conformation of the *A-B* methine bridge, the same geometry was predicted for the phytochromobilin chromophore in the Pr state of plant phytochromes on the basis of resonance Raman (RR) spectroscopy and density functional theory calculations (5).

For both classes of phytochromes, RR spectroscopy has shown that the respective Pr and Pfr forms contain a protonated (cationic) chromophore (6, 7). These results are in agreement with conclusions from Fourier transform infrared spectroscopy experiments with oat phytochrome (8) and have been confirmed by NMR studies on the cyanobacterial phytochrome Cph1 (9). Previous RR experiments with pea phytochrome suggested that the Pr → Pfr photoconversion involves a transient deprotonation of the chromophore in the formation of a meta-R-like ("bleached") intermediate (10). Together with stationary pH electrode measurements of different fragments of pea phytochrome (11) these results have been interpreted in terms of sequential proton release and uptake in the Pr → Pfr pathway where proton release is associated with the deprotonation of the chromophore (10). However, no kinetic evidence for this reaction scheme was provided, and the reprotonation of the chromophore in the formation of Pfr was not included. The proposed model remained thus speculative. In a recent study on the BV binding phytochrome Agp1 from *Agrobacterium tumefaciens* it was conclusively demonstrated by RR spectroscopy and flash photolysis that deprotonation of the tetrapyrrole in the meta-Rc state, the precursor of Pfr, is coupled to the release of a proton to the external medium, followed by reprotonation of the chromophore and proton re-uptake upon Pfr formation (7). Transient proton release and uptake could also be observed in the Pr → Pfr photoconversion of Cph1 (12). These findings suggest that proton translocations in the chromophore binding pocket are of fundamental importance for the Pr → Pfr photoconversion and specifically for the final reaction step of the Pfr formation. For a recent review on proton transfer in phytochrome see Ref. 13.

The crystal structure (4) shows that many amino acids in the binding pocket form a hydrogen bonding network with the chromophore and two water molecules (Fig. 10). The goal of the present work is to analyze the structural and functional role of the 2 highly conserved amino acids Asp-197 and His-250 that are hydrogen bonded to the chromophore. For this purpose the mutants D197A and H250A were prepared and characterized. A H250A mutant of full-length Agp1 has been characterized by UV-visible spectroscopy (14); plant, bacterial, and cyanobacterial phytochromes in which the histidine has been mutagenized have been described (15–18). A mutant of cyanobacterial phytochrome Cph1 in which the Asp-207 homolog was exchanged has also been described (18). The present work shows that in both Agp1 mutants the protonation of the Pr chromophore is affected, that the photoconversion is incomplete, and that the chromophore of the photoproducts is deprotonated. In this respect, the mutant photoproducts are different from that of the wild type, *i.e.* Pfr, which has a protonated chromophore (7).

EXPERIMENTAL PROCEDURES

Sequence Alignment and Analysis of Hydrogen Bonding—The selection of 46 protein sequences of phytochrome homologs was identical to that of a phylogenetic study published earlier (2). Protein alignments were performed using ClustalX, version 1.8 (19), with the "gap opening" and "gap extension" parameters set to 50 and 0.5, respectively. Potential hydrogen bonds were analyzed using the program HBPLUS (20) as implemented in the program LIGPLOT (21).

Cloning of Agp1-M15 and Mutants, Protein Expression and Purification—Cloning of the *Escherichia coli* expression vector pAG1-M15 was described previously (22). This vector encodes for a truncated version of Agp1 that lacks the histidine kinase and has additional histidines at its C terminus for affinity purification. The D197A and H250A mutants were cloned with the QuikChange site-directed mutagenesis kit (Stratagene) according to the instructions of the manufacturer. The mutations were confirmed by sequencing. For protein expression, 4-liter *E. coli* cultures were grown, collected, and extracted as described (22). Following affinity purification, the apoprotein was concentrated by ammonium sulfate precipitation and stored at concentrations of ~20 mg/ml in a buffer containing 300 mM NaCl, 50 mM Tris/Cl, 5 mM EDTA, pH 7.8, at −80° until further use. To this solution, 2 mM dithiothreitol (final concentration) and BV (5 mM methanol stock solution; Frontier Scientific, Carnforth, UK) were added. Unless indicated otherwise, the final molar concentration of BV was ~50% higher than that of the protein. After completion of assembly, the holoprotein was passed over a NAP desalting column (GE Healthcare) to remove free chromophore and residual ammonium sulfate and to allow for buffer exchange. The final buffer was 300 mM NaCl, 50 mM Tris/Cl, 5 mM EDTA, pH 7.8; for flash photolysis and transient protonation measurements, phytochrome was dissolved in 50 mM NaCl, pH 7.8. The holoprotein assembly kinetics was monitored by UV-visible spectroscopy as described (23).

Assembly and Photoconversion—The absorbance increase at 700 nm was monitored after mixing 7 μM biliverdin, 2 mM dithiothreitol with 14 μM apoprotein (final concentrations) at 18 °C. For photoconversion, the sample was irradiated with red light of 655 nm/50 μmol m^{-2} s^{-1} from a light-emitting diode for 2 min.

Flash Photolysis and Protonation Kinetics—Flash photolysis measurements were performed as described for full-length Agp1 (7). Photoconversion was induced by a 695-nm 10-ns laser flash and monitored at various wavelengths in the Soret (360–450 nm) and Q-band (600–800 nm) regions. The samples were used for repetitive measurements. Before each laser flash, the accumulation of the Pr state of Agp1-M15 wild-type and D197A samples was increased by irradiation with 784-nm light (7) and dark reversion, respectively. Because of the low dark conversion rate single flash traces were acquired for H250A; each sample was exposed to six flashes at most. Photoinduced proton exchange with the external medium was monitored by using appropriate pH indicator dyes as described (7, 12).

Stopped-flow Measurements—Stopped-flow-induced pH jumps were performed as described (24, 25). The mixing unit

(SHU-61; Hi-Tech, Salisbury, UK) had a dead time <2 ms. The D197A mutant was initially suspended in 5 mM Tris buffer at pH 6.5. After 1:1 mixing with 100 mM Tris, pH 8.0, the final measured pH was 7.9.

Resonance Raman Spectroscopy—RR spectra were measured at −140 °C using liquid nitrogen-cooled cryostats as described previously (7, 26). The protein concentration was ~200 mg/ml (50 mM Tris/Cl, 5 mM EDTA, 300 mM NaCl, pH 7.8). The energetic proximity of the 1064-nm excitation line with respect to the Q-band electronic transition of tetrapyrroles provides a substantial (pre-)resonance enhancement of the Raman bands of the chromophores in the Pr and Pfr states such that contributions from the apoprotein remain negligibly small. Only for phytochrome states with reduced Q-band oscillator strengths such as the meta-Rc intermediate is the resonance enhancement lower and Raman bands from the apo-protein (*e.g.* at 1450 and 1650 cm^{-1}) become detectable (7). The total accumulation time of each spectrum was ~2 h. In all RR spectra shown in this work, a linear background was subtracted. When necessary, residual spectral contributions from Pr or Pfr were also subtracted.

RESULTS AND DISCUSSION

Truncation and Mutations of Agp1—All experiments of the present study were performed with recombinant, affinity-purified Agp1-M15, which lacks the C-terminal histidine kinase module and comprises the N-terminal 504 amino acids with the PAS (named for period, aryl hydrocarbon receptor nuclear translocator and single-minded proteins) (27), GAF (named for cGMP-specific phosphodiesterase, adenylate cyclase, and Fhl proteins) (28), and PHY (specific for photochromic phytochromes) domains and additional 6 C-terminal histidine residues for affinity purification (22). For both the Pr and Pfr state, UV/visible and RR spectra of Agp1-M15 are identical to those of the Agp1 full-length protein (7, 22, 29). This agreement also holds for the photoconversion intermediates and kinetics studied in flash photolysis experiments, which reveal three components with time constants similar to those of the full-length protein, *i.e.* 350 μs, 3.6 ms, and 290 ms for the lumi-R → meta-Ra, meta-Ra → meta-Rc, and meta-Rc → Pfr transition, respectively. Like the full-length protein, Agp1-M15 shows transient proton release and uptake that are linked to the formation of meta-Rc and Pfr, respectively. Thus, these findings indicate that the histidine kinase module has only negligible influence on the spectral properties and the photoconversion kinetics of Agp1 such that the truncated Agp1-M15 is referred to as "wild-type" protein.

The crystal structure of the CBD of DrBphP (4) showed that 22 amino acids are located at a distance of <4 Å to the chromophore. Among them, Asp-207, His-260, and His-290 are of particular interest with respect to chromophore protonation. In phycocyanin (30), which is spectrally similar to the Pr form of phytochromes (31), the carboxylate side chain of an aspartate residue serves as a counterion for the protonated PCB chromophore. Histidine residues play important roles in the differential chromophore protonation of sensory rhodopsin (32). An alignment of 46 phytochrome protein sequences (2) showed that all 3 amino acids are conserved in 44 or 45 of the selected homologs, including Agp1. The present work is focused on

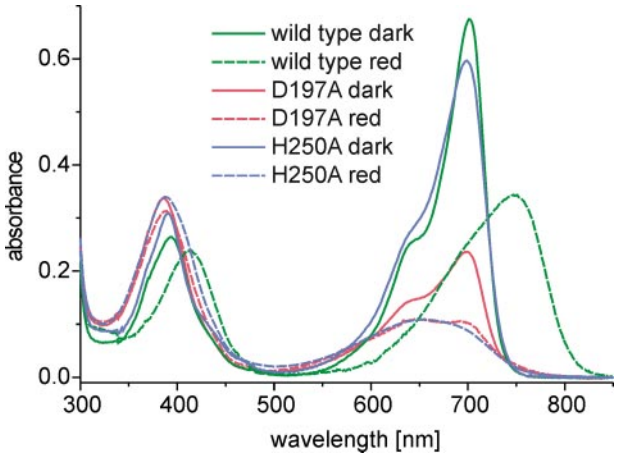

FIGURE 1. **UV-visible spectra of Agp1-M15, D197A, and H250A mutants at pH 7.8 before and after photoconversion.** The concentrations of the protein and BV were 14 and 7 μM, respectively. For each sample, one spectrum was recorded after completion of assembly and a second spectrum after photoconversion by 2 min of red light of 655 nm at 50 μM m^{-2} s^{-1}.

Asp-197 and His-250 of Agp1, which are homologous to Asp-207 and His-260 of DrBphP.

For the present work, we generated both the D197A and the H250A mutants of Agp1-M15. Both mutants incorporated the BV chromophore in a covalent manner, although their assembly rates were significantly reduced. In the wild-type protein, the slow component of the assembly kinetics (24) is associated with a time constant of less than 20 s, whereas for H250A and D197A the time constants have been determined to be 2 and 20 min, respectively (data not shown).

The absorption spectrum of the D197A mutant differs significantly from that of the wild type. Specifically, the intensity ratio of the Q (~700 nm) and Soret (~380 nm) absorption bands in the UV-visible spectrum, typically 2:1 in the wild-type protein, is reversed (Fig. 1). On the other hand, the absorption spectrum of the H250A mutant in the Pr state is similar to that of the wild type except for a slight broadening of the Q-band and an increase of the Soret band (Fig. 1). Thus, the Pr spectrum of H250A is intermediate between that of the wild type and D197A. The H250A mutant displays the same spectral and photoactive properties as its full-length version (14).

Protonation of the Chromophore in the Pr State—The absorption spectra of the Pr form of the wild type and both mutants are strongly pH dependent, in particular in the Q-band (see Fig. 2, *A–C*). Analyzing the pH dependence of the UV-visible absorption spectra on the basis of the Henderson-Hasselbalch equation, pK_a values of 7.2, 8.8, and 11.1 were determined for D197A, H250A, and the wild-type protein, respectively (Fig. 2*D*). The respective Hill coefficients of 0.85, 1.02, and 0.81 suggest that one proton is involved. Similar spectrophotometric titration experiments with the cyanobacterial phytochrome Cph1 led to a pK_a value of 9.5 (12), which was attributed to the deprotonation of the PCB chromophore on the basis of a comparison with the pH-dependent spectra of the model compound octaethylbiliverdin (33). Here we show by RR spectroscopy that in Agp1 the underlying acid-base reaction is also linked to the deprotonation of the chromophore (Fig. 3). The RR spectra of protonated (cationic) linear methine-bridged tet-

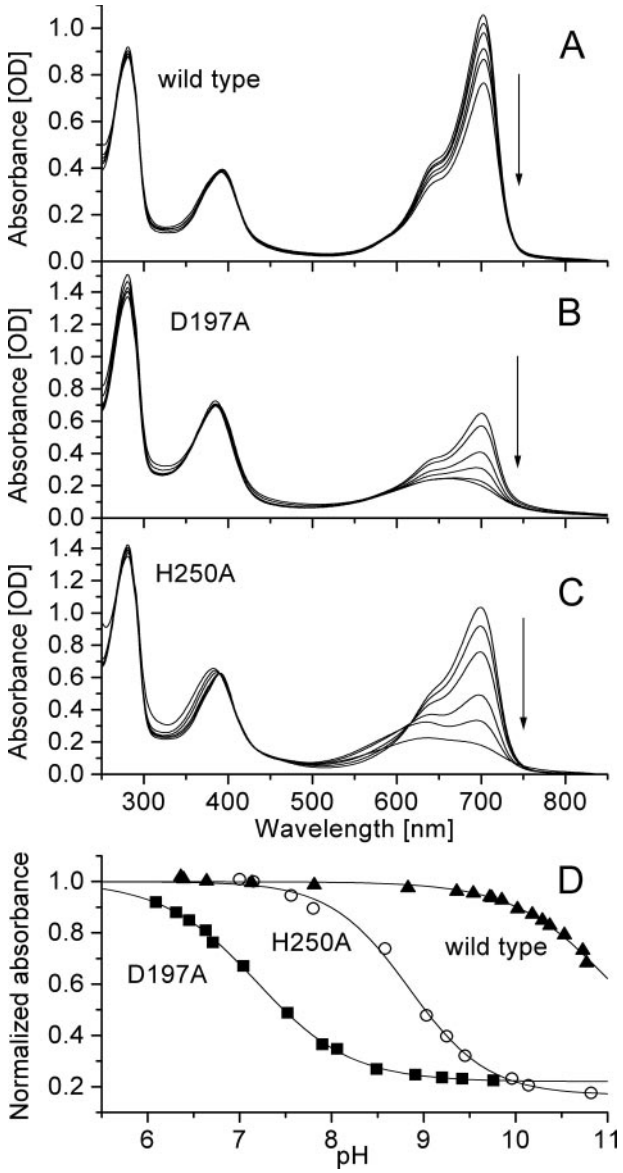

FIGURE 2. *A*, absorption spectra of wild-type (Agp1-M15) at pH 6.4, 8.85, 9.75, 10.2, 10.35, and 10.75. *B*, absorption spectra of D197A at pH 6.7, 7.05, 7.5, 7.9, 8.5, and 9.1. *C*, absorption spectra of H250A at pH 7.0, 7.8, 8.6, 9.05, 9.45, and 10.8. The *arrows* in *panels A–C* indicate the direction of the decrease of absorption in the Q-bands with increasing pH. *D*, titration curves of Agp1-M15, D197A, and H250A. The normalized absorption at λ_{max} of the Q-band is plotted as a function of pH. The Henderson-Hasselbalch equation was fitted to the data with pK_a values of 7.2, 8.8, and 11.1 and Hill coefficients of 0.85, 1.02, and 0.81 for D197A, H250A, and Agp1-M15, respectively. For the wild-type protein, the normalized absorbance at high pH was set to 0.2.

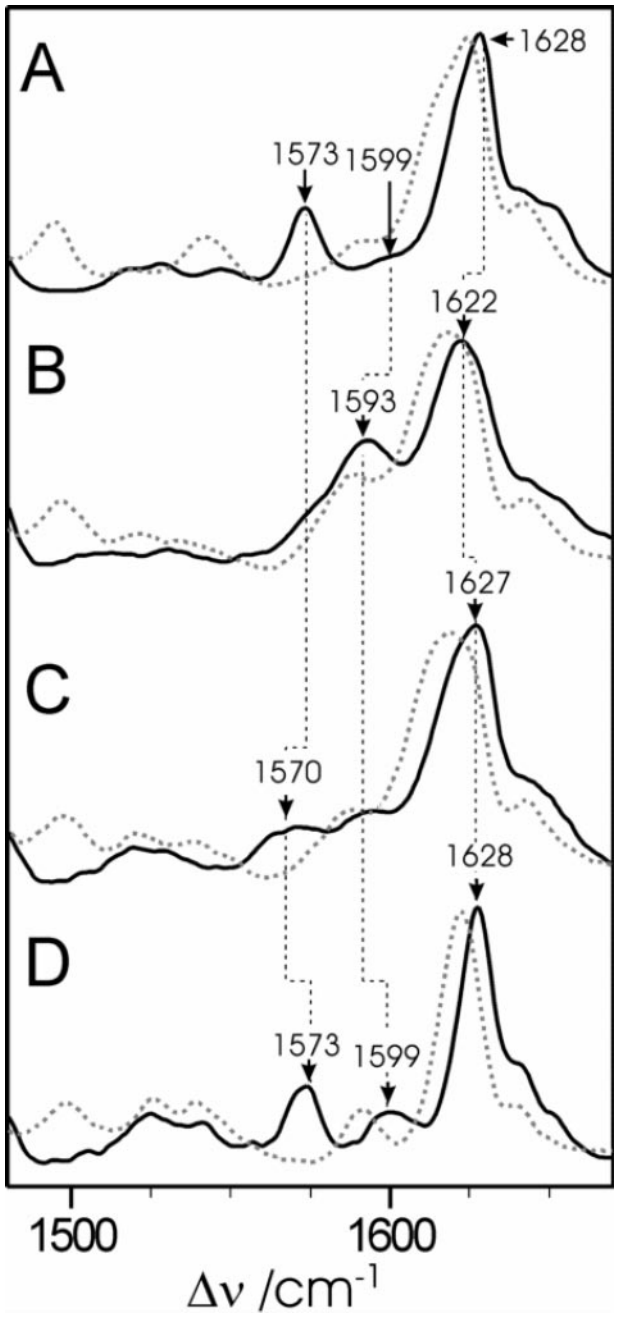

FIGURE 3. **RR spectra of the Pr states of wild-type Agp1-M15 at pH 7.8 (*A*), D197A at pH 7.8 (*B*), D197A at pH 6.3 (*C*), and H250A at pH 7.8 (*D*) measured at −140 °C.** The *solid* and *dotted lines* refer to the spectra measured in H_2O and D_2O, respectively. Broad range spectra are shown in supplemental Figs. S1 and S2.

rapyrroles display a band between 1580 and 1550 cm^{-1} that originates from the N-H in-plane (ip) bending of the ring *B* and *C* N-H groups (6). In wild-type Agp1-M15 (pH 7.8), this band is found at 1573 cm^{-1} and it disappears upon H/D exchange (Fig. 3*A*) (7). The corresponding N-D ip mode is observed at 1078 cm^{-1} (supplemental Figs. S2 and S3). The intensity of the N-H ip mode is strongly reduced in the spectrum of the D197A mutant measured at a pH of 7.8, implying that the chromophore is largely in the non-protonated (neutral) form as expected from the pK_a value of 7.2 (Fig. 3*B*). Correspondingly, a substantial fraction of the chromophore is protonated at pH 6.3 as indicated by the N-H ip mode at 1570 cm^{-1}, which disappears in D_2O (Fig. 3*C*). The pH-dependent protonation of the chromophore is also reflected by the intensity increase of the N-D ip from pH 7.8 to pH 6.3 (supplemental Fig. S3). For H250A (pK_a = 8.8) the chromophore is expected to be largely protonated at pH 7.8 as confirmed by the RR spectrum (Fig. 3*D*). The fraction of the protonated chromophore is identified on the basis of the N-H ip mode (1573 cm^{-1}), which shifts down to 1080 cm^{-1} in D_2O, whereas the smaller fraction of the unprotonated chromophore is reflected by the increased intensity at 1599 cm^{-1} as compared with the wild-type protein. This band is assigned to the C = C stretching mode of the methine

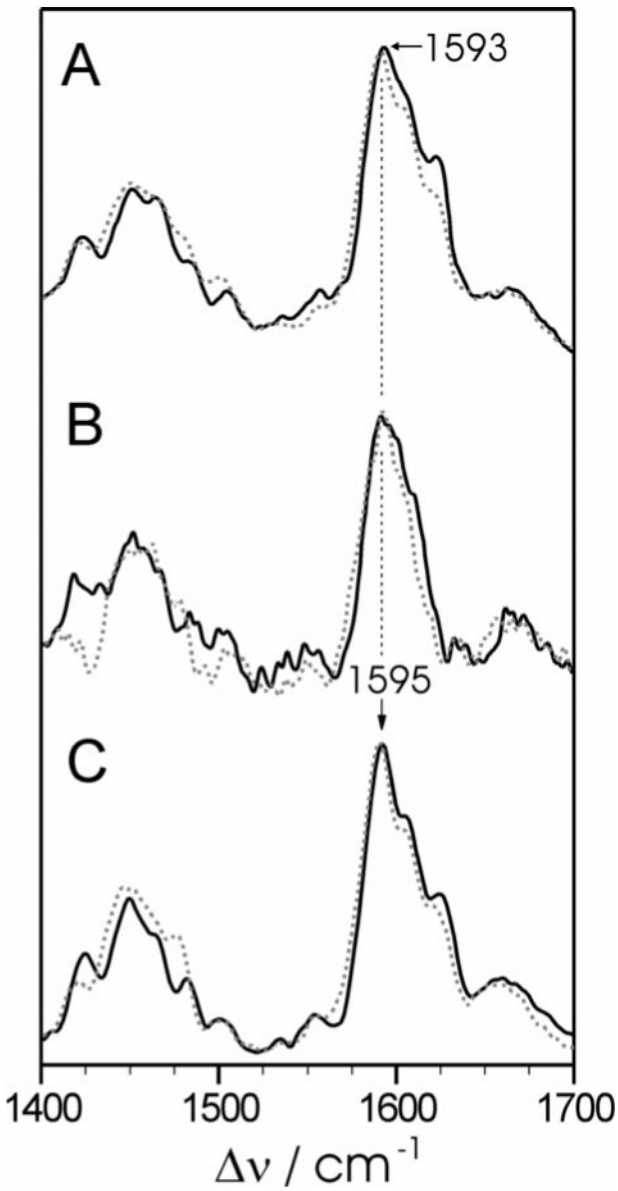

FIGURE 4. **RR spectra of the photoconversion products of D197A (*B*) and H250A (*C*) compared with the spectrum of the meta-Rc (*A*) state of wild-type Agp1, all measured at pH 7. 8 and −140 °C.** The *solid* and *dotted lines* refer to the spectra measured in H_2O and D_2O, respectively.

bridges of the non-protonated chromophore and corresponds to the strong 1593 cm^{-1} band of the D197A mutant at pH 7.8. The direction of the pK_a shift in D197A suggests that the negatively charged group of Asp-197 serves as the counterion of the chromophore. The structure of the CBD of DrBphP shows, however, that at least in that smaller crystalline fragment, the Asp-197 side chain points outward away from the chromophore (4).

Photoconversion—Upon irradiation of D197A and H250A with red light, the absorbance of the Q-band is further reduced (Fig. 1). A similar reduced Q-band intensity has also been observed in the UV-visible absorption spectrum of the cryo-trapped meta-Rb intermediate of oat phytochrome, which is in equilibrium with meta-Rc (34). In contrast to the wild-type meta-Rc state (7), the photoconversion products of the mutants do not display the characteristic 50–60-nm red-shift of the Q-band with respect to the Pr state. However, the RR spectra of

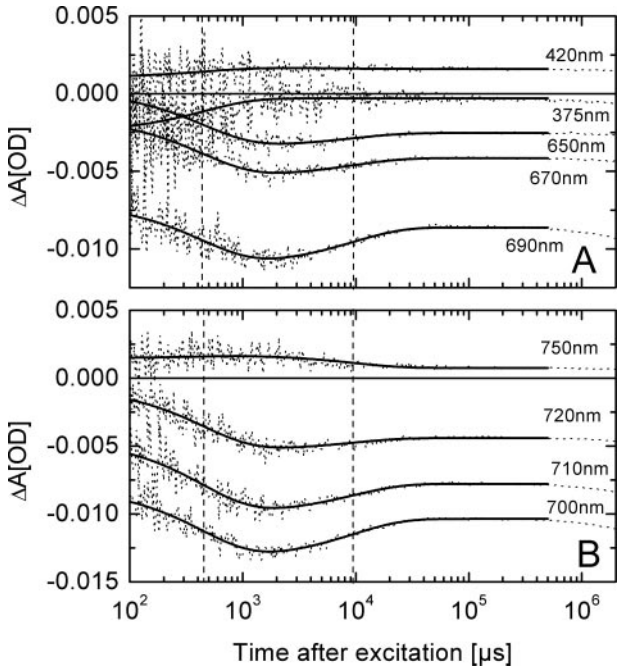

FIGURE 5. ***A* and *B*, transient absorption changes of D197A (pH 6. 5, 20 °C) measured at the indicated wavelengths after laser flash excitation at 695 nm (*dotted lines*).** The data were fitted simultaneously from 100 μs to 500 ms to a sum of two exponentials (*thick solid lines*) with time constants of 460 μs and 10 ms as marked by *vertical dashed lines*.

the photoproducts of both D197A and H250A display far reaching similarities with that of the meta-Rc intermediate of wild-type Agp1 (7). In the cryogenically trapped meta-Rc state the chromophore is deprotonated as indicated by the lack of the N-H in-plane bending mode as well as by the prominent and broad band at 1593 cm^{-1} that is largely H/D insensitive (Fig. 4*A*) (35). This characteristic pattern is also observed in the RR spectra of the photoconversion products of both mutant proteins. These findings indicate that the chromophore is unprotonated and adopts largely the same *ZZE* geometry as in the meta-Rc state of the wild-type protein. The small differences in the RR spectra of the three species (see Fig. 4 and supplemental Fig. S4) most likely reflect differences in the cofactor-protein interactions brought about by the substitution of Asp-197 and His-250 in the chromophore pocket.

Kinetics of Photoconversion and Protonation Changes—Flash photolysis measurements of the D197A adduct at pH 6.5, *i.e.* at nearly complete protonation of the chromophore, reveal transient absorption changes at 700 nm that are about five times lower than those observed for the wild-type protein (Fig. 5) and decrease even further with increasing pH (Fig. 6*A*). This finding is consistent with an ~5-fold lower rate of photoconversion under continuous illumination (data not shown) indicating an ~5-fold lower photoconversion quantum efficiency of the dark state of D197A with respect to that of wild type. The initial (unresolved) absorption changes of D197A ($t \leq 50$ μs) are different from those of the wild-type because they lack positive signals for $\lambda > 720$ nm that are characteristic of the lumi-R intermediate. Simultaneous exponential fits to the time traces at 9–10 different wavelengths revealed two kinetic components with time constants of 300–500 μs (τ_1) and 10–20 ms (τ_2), respectively (Fig. 5). The first component is associated with

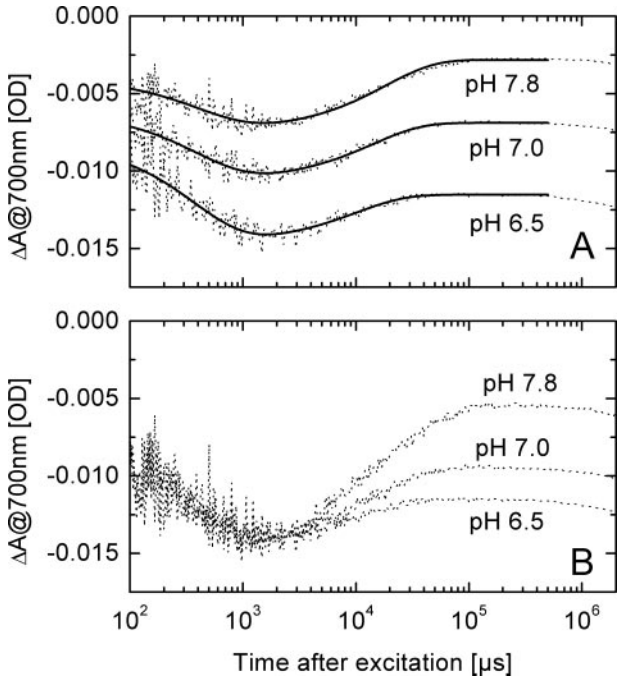

FIGURE 6. *A*, transient absorption changes of D197A at the indicated pH values (20 °C) measured at 700 nm after laser flash excitation at 695 nm (*dotted lines*). Each trace was fitted from 100 μs to 500 ms to a sum of two exponentials (*thick solid lines*) with time constants of 430 μs and 18 ms (pH 7.8), 410 μs and 14 ms (pH 7.0), and 390 μs and 10 ms (pH 6.5), respectively. *B*, traces from *panel A* scaled to the same bleach at ~2 ms. The relative amplitude of the second component (10–18 ms) increases with increasing pH according to the pK_a value of 7.2 of the protonation equilibrium in the dark state.

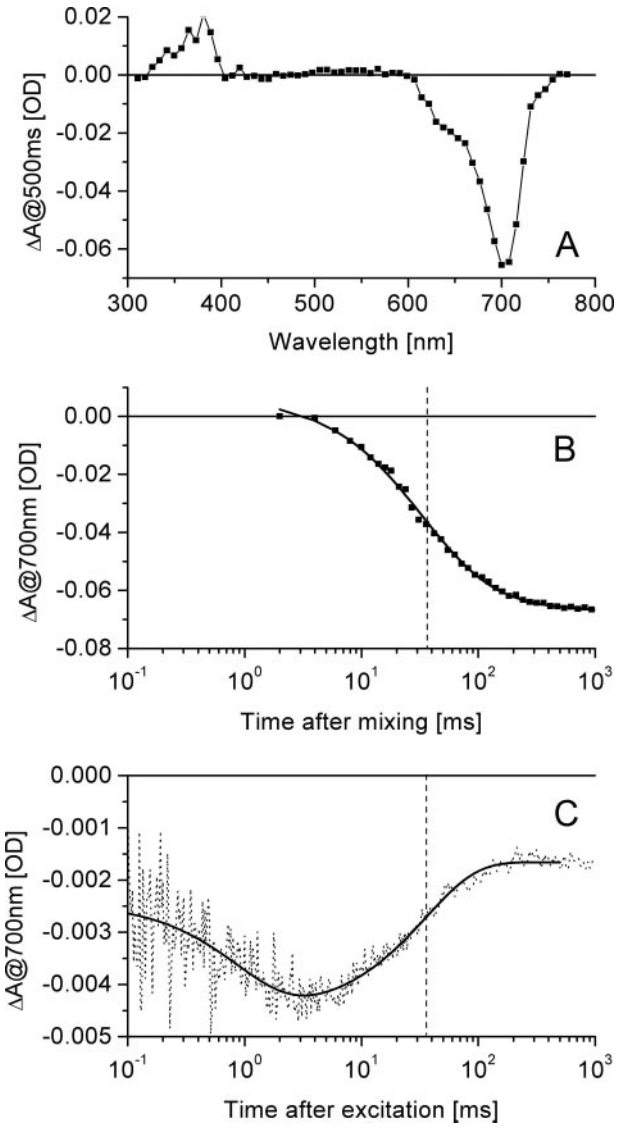

FIGURE 7. *A* and *B*, stopped-flow relaxation kinetics of the protonation equilibrium in the dark state of D197A after a pH jump from 6.5 to 7.9. The data are averages of over nine shots. *A*, spectral changes at 500 ms with respect to 2 ms after mixing. *B*, kinetics of the transient absorption changes at 700 nm. *C*, kinetics of the transient absorption change at 700 nm after laser flash excitation at 695 nm for the same sample as in *panels A* and *B* after a pH jump (pH 7.9). The vertical line in *panels B* and *C* marks the common time constant of 35 ms. Conditions: 50 mM Tris (final concentration), 50 mM NaCl, 10 °C.

positive amplitudes and reflects the formation of the photoconversion product. The second component displays negative amplitudes (10–20 ms) that increase with increasing pH (Fig. 6). As confirmed by stopped-flow pH jump experiments (Fig. 7), this component is due to the relaxation of the protonation equilibrium of the chromophore in the dark state (Pr) that is perturbed by the flash-induced depletion of the protonated species. The kinetics of the transient absorption changes at 700 nm after a pH jump from pH 6.5 to 7.9 (Fig. 7*B*) is virtually the same as that of the second component of the 700-nm signal after laser flash excitation at pH 7.9 (Fig. 7*C*). These results strongly support the existence of the protonation equilibrium and imply that only the protonated species undergoes a photoreaction with moderate efficiency. A similar phenomenon has been observed with the photoreceptor photoactive yellow protein (25).

The photo-induced processes of the mutant H250A at pH 7.8 (Fig. 8*A*) are more similar to wild-type Agp1 (see Ref. 7) as indicated by the comparable amplitudes of the transient absorption changes at 700 nm and the same spectral characteristics of the initial absorption changes (lumi-R). Furthermore, the kinetics of the biphasic formation of the H250A photoconversion product (τ_1 = 270 μs, τ_2 = 2.0 ms) are similar to that of the meta-Rc intermediate in wild type (7). The relative amplitude of the 50-ms component (τ_3), which in D197A was attributed to the relaxation of the protonation equilibrium in the Pr state (Fig. 5*B*), is very small at pH 7.8 for H250A (Fig. 8*A*) and thus in line with the pK_a of 8.8. Whereas transient protonation changes could not be observed with D197A at any pH, H250A displayed proton release with a time constant of 1.1 ms (Fig. 8*B*), which is very close to τ_2 and comparable with the wild-type proton release time of ~3 ms (7). The absence of a subsequent proton uptake phase in H250A is consistent with the inhibition of the formation of Pfr. Though the spectrum of the photoproduct in H250A differs from that of meta-Rc in wild type (red-shift is missing), the protonation signal and the similarity of the time constants suggest that the photoproduct of H250A is a meta-Rc-like state.

Protein Structural Changes during the Photoconversion—On the basis of size exclusion chromatography it has been demonstrated that the Pfr state of Agp1-M15 has a higher mobility than the Pr state. This observation has been related to a substantial conformational change of the apoprotein induced by the photoconversion (29). For the Pr states of the D197A and H250A mutants, this assay reveals slightly different mobilities

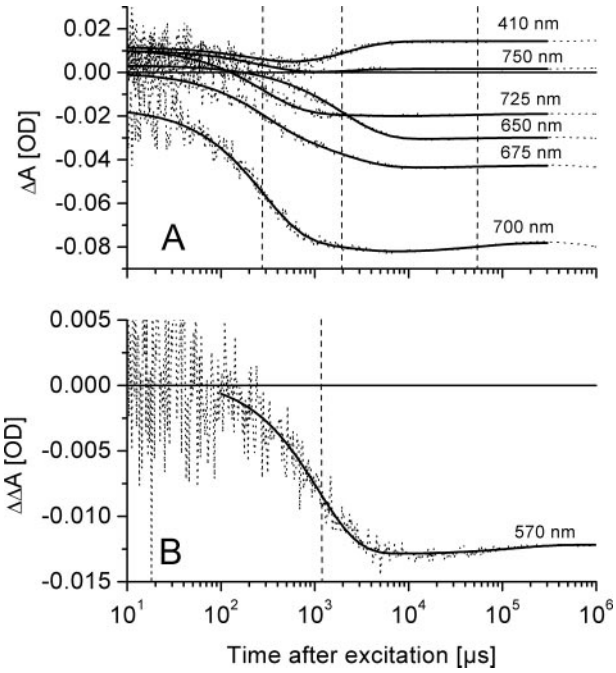

FIGURE 8. *A*, transient absorption changes of H250A (pH 7. 8) measured at the indicated wavelengths after laser flash excitation at 695 nm (*dotted lines*). The data were fitted simultaneously from 10 μs to 300 ms to a sum of three exponentials (*thick solid lines*) with time constants of 280 μs, 2.0 ms, and 50 ms as marked by *vertical dashed lines*. *B*, dye signal (cresol red) after flash excitation of H250A corrected for contributions of the chromoprotein (*dotted line*). The trace was fitted to a sum of two exponentials (*thick solid line*) with time constants of 1.1 ms (proton release component marked by *vertical dashed line*) and 140 ms.

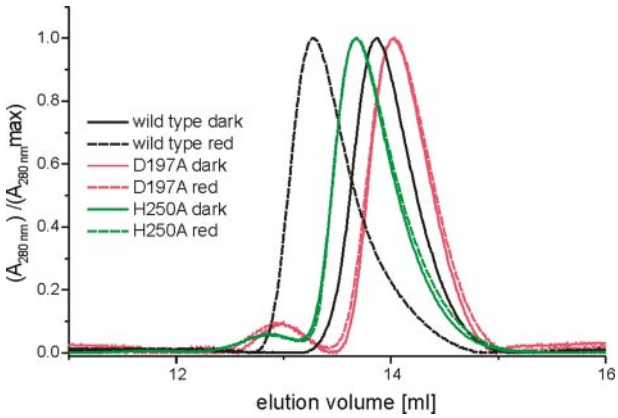

FIGURE 9. **Size exclusion chromatography of the wild-type protein, D197A, and H250A.** Each holoprotein was assayed before and after photoconversion.

as compared with the wild-type protein, pointing to subtle effects of the mutations on the global fold of the protein (Fig. 9). However, no light-induced changes of the mobilities are observed in either mutant. Hence, the major protein conformational changes that are associated with the Pr → Pfr photoconversion in the wild-type protein occur during the transition from meta-Rc to Pfr, *i.e.* in the step that is blocked in the mutant proteins.

Structural and Mechanistic Implications—In total, 16 of 22 amino acids that are within a distance of 4 Å from BV are identical in DrBphP and Agp1. Because of this high degree of homology, the structure of the chromophore pocket and the hydrogen bond network are likely to be similar in Agp1 and

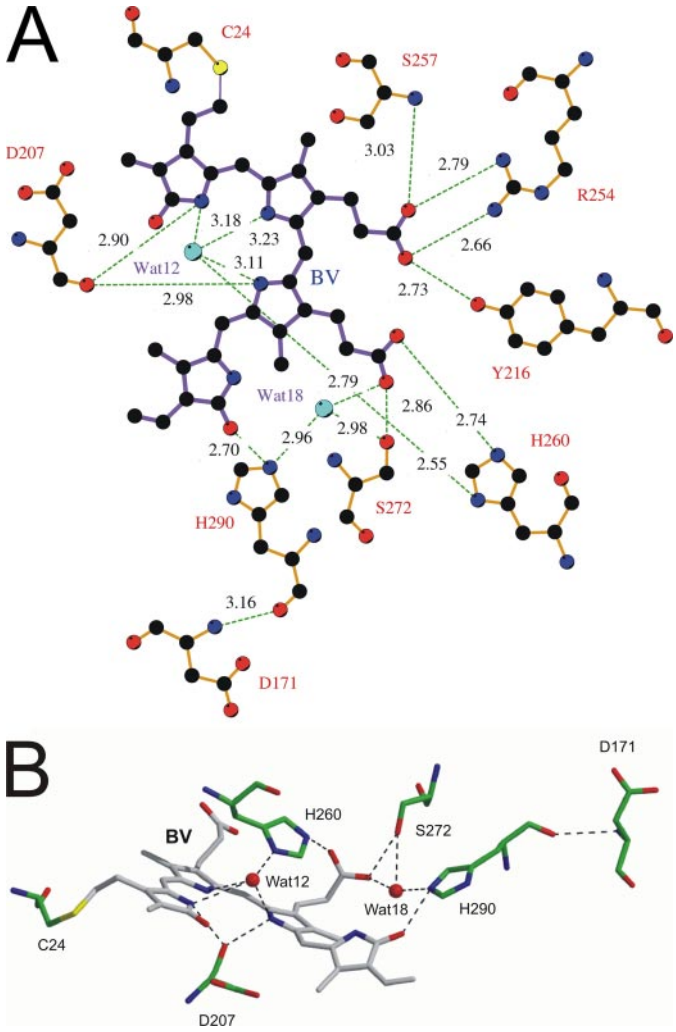

FIGURE 10. **Potential hydrogen bond networks involving BV of the CBD of DrBphP according to the PDB entry 1ZTU (4).** *A*, schematic view, drawn using LIGPLOT (21). The amino acids Asp-171, Asp-207, Tyr-216, Arg-254, Ser-257, His-260, Ser-272, and His-290 of DrBphP that are involved in the network are presented. The Agp1 homologs are Asp-161, Asp-197, Tyr-206, Arg-244, Ser-247, His-250, Ser-262, and His-280, respectively. *B*, three-dimensional arrangement of the BV chromophore and its hydrogen bonding partners in the first network into which the nitrogen atoms of the pyrrole rings are embedded. The second hydrogen network involving the propionate side chain of pyrrole ring B has been omitted for clarity, as it is separated from the first. The figure was drawn using MOLSCRIPT (37) and RASTER3D (36).

DrBphP. In the structural model of the CBD of DrBphP (4), the amino acids Asp-207 and His-260 (homologous to Asp-197 and His-250 in Agp1) are positioned close to the ring *B* and *C* nitrogens of the chromophore. Analysis of the potential hydrogen bond interactions in the CBP by means of the programs HBPLUS (20) and LIGPLOT (21) reveals the tetrapyrrole chromophore to be embedded in two independent hydrogen bond networks (Fig. 10*A*). Only the first network, which is the more extended one comprising 5 amino acids and 2 water molecules together with the chromophore, involves the BV pyrrole rings (Fig. 10*B*). The nitrogen atoms of the BV pyrrole rings *A*, *B*, and *C* form hydrogen bonds with a water molecule (Wat12), which in turn is linked by a hydrogen bond to the δ1 nitrogen of His-260. The ϵ2 N-H group of His-260 forms a hydrogen bond to an oxygen of the ring *C* propionic side chain, whereas the other oxygen is linked to Ser-272 and His-290 via Wat18. The ϵ2 N-H

group of His-290 also interacts with the carbonyl group of ring *D* of BV. The N-H groups of the BV rings *B* and *C* are in hydrogen bond distance with the carbonyl oxygen of Asp-207.

As shown in this work, both Asp-197 and His-250 of Agp1 are important for stabilizing the protonation of the inner pyrrole rings of the chromophore. The finding that the backbone carbonyl of Asp-207 of DrBphP, and not the anionic side chain, forms a hydrogen bond contact to the ring *B* and *C* N-H groups of BV is in contrast to the situation in phycocyanin. In this case, the carboxyl group of an Asp serves as a counterion for the chromophore (30). The rather low pK_a value of D197A of Agp1 suggests that the carboxyl side group of Asp-197 also functions as counterion for the chromophore in Agp1. Upon inspection of the crystal structure of DrBphP it becomes evident that in one of three possible rotamer positions obtained by rotations of the C_α–C_β bond, the carboxyl group of Asp-207 is located at a hydrogen bonding distance of 3.3 Å to Wat12. This conformation is unlikely in the Pr state because it causes a steric clash with the ring D methyl side chain of BV, although it cannot be ruled out for the protein in solution. Notably, this sterical hindrance is removed for the *ZZE* isomer of the chromophore, *i.e.* for the lumi-R primary photoproduct and thereafter. This observation suggests that conformational changes of Asp-207 (Asp-197 in Agp1) might be actively involved in the mechanism of transient deprotonation and reprotonation of the chromophore along the photocycle.

Only the protonated chromophore undergoes the photo-induced *Z-E* isomerization of the *C-D* methine bridge in the first step of the Pr → Pfr conversion. The rotation around the double bond causes the rupture of the hydrogen bond between ring *D* and His-290 of DrBphP (homologous to His-280 in Agp1) and may induce further rearrangements of the hydrogen bond network during the subsequent thermal relaxations of the chromophore. As a result, the deprotonation of the chromophore is facilitated in the meta-Rc state. In the formation of this state, deprotonation of BV leads to the release of a proton to the external medium in both the wild-type protein and the H250A mutant. A similar mechanism had been suggested earlier for pea phytochrome (10). The lack of proton release (and uptake) in D197A of Agp1 suggests that Asp-197 serves as the proton release group by transient exposure of its carboxyl side chain in meta-Rc. In the wild-type protein, proton re-uptake occurs in the final reaction step of the Pr → Pfr photoconversion, *i.e.* the meta-Rc → Pfr transition (7), which is inhibited in D197A and H250A. We therefore conclude that the reversible Asp-197-mediated proton transfer between the chromophore and the external medium is intimately linked to the quite substantial chromophore and protein structural rearrangements associated with the formation of the Pfr state. It may be that the transient proton translocation represents a trigger for these structural changes. The lack of proton re-uptake and Pfr formation in H250A then suggests that His-250 is directly involved in these conformational changes that complete the conversion to the Pfr state.

Acknowledgments—We thank Olga Butova and Maike Mette for help with protein purification and Katrina Forest for helpful discussions.

REFERENCES

1. Briggs, W. R., and Spudich, J. L. (eds) (2005) in *Handbook of Photosensory Receptors*, Wiley Press, Weinheim, Germany
2. Lamparter, T. (2004) *FEBS Lett.* **573,** 1–5
3. Tu, S. L., and Lagarias, J. C. (2005) in *Handbook of Photosensory Receptors* (Briggs, W. R., and Spudich, J. L., eds) pp. 121–149, Wiley Verlag, Weinheim, Germany
4. Wagner, J. R., Brunzelle, J. S., Forest, K. T., and Vierstra, R. D. (2005) *Nature* **438,** 325–331
5. Mroginski, M. A., Murgida, D. H., von Stetten, D., Kneip, C., Mark, F., and Hildebrandt, P. (2004) *J. Amer. Chem. Soc.* **126,** 16734–16735
6. Kneip, C., Hildebrandt, P., Schlamann, W., and Braslavsky, S. E. (1999) *Biochemistry* **16,** 15185–15192
7. Borucki, B., von Stetten, D., Seibeck, S., Lamparter, T., Michael, N., Mroginski, M. A., Otto, H., Murgida, D. H., Heyn, M. P., and Hildebrandt, P. (2005) *J. Biol. Chem.* **280,** 34358–34364
8. Foerstendorf, H., Mummert, E., Schäfer, E., Scheer, H., and Siebert, F. (1996) *Biochemistry* **35,** 10793–10799
9. Strauss, H. M., Hughes, J., and Schmieder, P. (2005) *Biochemistry* **44,** 8244–8250
10. Mizutani, Y., Tokutomi, S., and Kitagawa, T. (1994) *Biochemistry* **33,** 153–158
11. Tokutomi, S., Yamamoto, K. T., and Furuya, M. (1988) *Photochem. Photobiol.* **47,** 439–445
12. van Thor, J. J., Borucki, B., Crielaard, W., Otto, H., Lamparter, T., Hughes, J., Hellingwerf, K. J., and Heyn, M. P. (2001) *Biochemistry* **40,** 11460–11471
13. Borucki, B. (2006) *Photochem. Photobiol. Sci.* **5,** 553–566
14. Lamparter, T., Carrascal, M., Michael, N., Martinez, E., Rottwinkel, G., and Abian, J. (2004) *Biochemistry* **43,** 3659–3669
15. Bhoo, S. H., Hirano, T., Jeong, H. Y., Lee, J. G., Furuya, M., and Song, P.-S. (1997) *J. Amer. Chem. Soc.* **119,** 11717–11718
16. Davis, S. J., Vener, A. V., and Vierstra, R. D. (1999) *Science* **286,** 2517–2520
17. Karniol, B., Wagner, J. R., Walker, J. M., and Vierstra, R. D. (2005) *Biochem. J.* **392,** 103–116
18. Hahn, J., Strauss, H. M., Landgraf, F. T., Faus Gimenez, H., Lochnit, G., Schmieder, P., and Hughes, J. (2006) *FEBS J.* **273,** 1415–1429
19. Thompson, J. D., Gibson, T. J., Plewniak, F., Jeanmougin, F., and Higgins, D. G. (1997) *Nucleic Acids Res.* **24,** 4876–4882
20. McDonald, I. K., and Thornton, J. M. (1994) *J. Mol. Biol.* **238,** 777–793
21. Wallace, A. C., Laskowski, R. A., and Thornton, J. M. (1995) *Protein Eng.* **8,** 127–134
22. Scheerer, P., Michael, N., Park, J. H., Noack, S., Förster, C., Hammam, M. A. S., Inomata, K., Choe, H. W., Lamparter, T., and Krauss, N. (2006) *J. Struct. Biol.* **153,** 97–102
23. Lamparter, T., Michael, N., Mittmann, F., and Esteban, B. (2002) *Proc. Natl. Acad. Sci. U. S. A.* **99,** 11628–11633
24. Borucki, B., Otto, H., Rottwinkel, G., Hughes, J., Heyn, M. P., and Lamparter, T. (2003) *Biochemistry* **42,** 13684–13697
25. Borucki, B., Otto, H., Joshi, C. P., Gasperi, C., Cusanovich, M. A., Devanathan, S., Tollin, G., and Heyn, M. P. (2003) *Biochemistry* **42,** 8780–8790
26. Matysik, J., Hildebrandt, P., Schlamann, W., Braslavsky, S. E., and Schaffner, K. (1995) *Biochemistry* **34,** 10497–10507
27. Ponting, C. P., and Aravind, L. (1997) *Curr. Biol.* **7,** R674–R677
28. Aravind, L., and Ponting, C. P. (1997) *Trends Biochem. Sci.* **22,** 458–459
29. Inomata, K., Hammam, M. A. S., Kinoshita, H., Murata, Y., Khawn, H., Noack, S., Michael, N., and Lamparter, T. (2005) *J. Biol. Chem.* **280,** 24491–24497
30. Schirmer, T., Bode, W., and Huber, R. (1987) *J. Mol. Biol.* **196,** 677–695
31. Arciero, D. M., Bryant, D. A., and Glazer, A. N. (1988) *J. Biol. Chem.* **263,** 18343–18349
32. Zhang, X. N., and Spudich, J. L. (1997) *Biophys. J.* **73,** 1516–1523
33. Mizutani, Y., Tokutomi, S., Aoyagi, K., Horitsu, K., and Kitagawa, T. (1991) *Biochemistry* **30,** 10693–10700
34. Eilfeld, P., and Rüdiger, W. (1985) *Z. Naturforsch. Sect. C-J. Biosci.* **40,** 109–114
35. Hildebrandt, P., Kneip, C., Matysik, J., Nemeth, K., Magdo, I., Mark, F., and Schaffner, K. (1999) *Rec. Res. Dev. Phys. Chem.* **3,** 63–77
36. Merritt, E. A., and Bacon, D. J. (1997) *Methods Enzymol.* **277,** 505–524
37. Kraulis, P. J. (1991) *J. Appl. Crystallogr.* **24,** 947–950